Radiation and Mass Transfer Effects on the Magnetohydrodynamic Unsteady Flow Induced by a Stretching Sheet

Tasawar Hayat[a], Muhammad Qasim[a], and Zaheer Abbas[b]

[a] Department of Mathematics, Quaid-I-Azam University 45320, Islamabad 44000, Pakistan
[b] Department of Mathematics, FBAS, International Islamic University, Islamabad 44000, Pakistan

Reprint requests to Z. A.; E-mail address: za_qau@yahoo.com

Z. Naturforsch. **65a,** 231 – 239 (2010); received March 10, 2009 / revised June 2, 2009

This investigation deals with the influence of radiation on magnetohydrodynamic (MHD) and mass transfer flow over a porous stretching sheet. Attention has been particularly focused to the unsteadiness. The arising problems of velocity, temperature, and concentration fields are solved by a powerful analytic approach, namely, the homotopy analysis method (HAM). Velocity, temperature, and concentration fields are sketched for various embedded parameters and interpreted. Computations of skin friction coefficients, local Nusselt number, and mass transfer are developed and examined.

Key words: Magnetohydrodynamic; Radiation; Concentration Field; Series Solutions.

1. Introduction

The classical problem of boundary layer flow bounded by a stretching surface has been studied extensively for viscous and non-Newtonian fluids. Good lists of relevant references on the topic can be seen in the recent studies [1 – 10] and several references therein. Examples of stretching flows are found in wire drawing, aerodynamic extrusion of plastic sheets, paper production, crystal growing, etc. Literature survey shows that much attention has been given to the stretching flows in steady situation. Little attention is given to the unsteady flows over a stretching surface [11 – 15]. Such flows are rarely discussed when interaction of magnetohydrodynamics and radiation is taken into account.

The main purpose of the present paper is to extend the analysis of Ishak et al. [15] in four directions. Firstly, to discuss the MHD effects. Secondly, to describe the influence of radiation. Thirdly, to analyze the interaction of MHD and radiation with mass transfer in chemical reacting fluid. Fourthly, to construct the series solutions by employing the homotopy analysis method [16 – 30]. The paper is organized as follows: The next section provides the problem of the development. Homotopy analysis solutions are derived in Section 3. Section 4 includes the convergence of the series solution. Sections 5 and 6, respectively, consist of discussion and main points.

2. Mathematical Formulation

Here we examine the unsteady and MHD flow of an incompressible viscous fluid bounded by a porous stretching surface. The fluid is electrically conducting under the influence of a time dependent magnetic field $B(t)$ applied in a direction normal to the stretching surface. The induced magnetic field is negligible under the assumption of a small magnetic Reynolds number. In addition, heat and mass transfer phenomena are considered. We choose the x-axis parallel to the porous surface and the y-axis normal to it. The boundary layer flow is governed by the following equations:

$$\frac{\partial u}{\partial x}+\frac{\partial v}{\partial y}=0, \tag{1}$$

$$\frac{\partial u}{\partial t}+u\frac{\partial u}{\partial x}+v\frac{\partial u}{\partial y}=\nu\frac{\partial^2 u}{\partial y^2}-\frac{\sigma B^2(t)}{\rho}u, \tag{2}$$

$$\rho c_{\mathrm{p}}\left[\frac{\partial T}{\partial t}+u\frac{\partial T}{\partial x}+v\frac{\partial T}{\partial y}\right]=k\frac{\partial^2 T}{\partial y^2}-\frac{\partial q_{\mathrm{r}}}{\partial y}, \tag{3}$$

$$\frac{\partial C}{\partial t}+u\frac{\partial C}{\partial x}+v\frac{\partial C}{\partial y}=D\frac{\partial^2 C}{\partial y^2}-R(t)C, \tag{4}$$

where u and v are the velocity components in the x and y-directions, respectively, ρ the fluid density, ν the kinematic viscosity, σ the electrical conductivity, T the temperature, c_{p} the specific heat, k the thermal conductivity of the fluid, q_{r} the radiative heat flux, D is the mass diffusion, C the concentration field, and $R(t)$ represents the reaction rate.

Employing the Rosseland approximation for radiation [31] one has

$$q_r = -\frac{4\sigma^*}{3k^*}\frac{\partial T^4}{\partial y}, \quad (5)$$

in which σ^* is the Stefan-Boltzmann constant and k^* the mean absorption coefficient. We express the term T^4 as the linear function of temperature into a Taylor series about T_∞ by neglecting higher terms, and write

$$T^4 \approxeq 4T_\infty^3 T - 3T_\infty^4. \quad (6)$$

From (3), (5), and (6) we have

$$\rho c_p \left[\frac{\partial T}{\partial t} + u\frac{\partial T}{\partial x} + v\frac{\partial T}{\partial y}\right] = \frac{\partial}{\partial y}\left[\left(\frac{16\sigma^* T_\infty^3}{3k^*} + k\right)\frac{\partial T}{\partial y}\right]. \quad (7)$$

The subjected boundary conditions are

$$u = U_w, \quad v = V_w, \quad T = T_w, \quad C = C_w \text{ at } y = 0, \quad (8)$$

$$u \to 0, \quad T \to T_\infty, \quad C \to C_\infty \text{ as } y \to \infty. \quad (9)$$

$$V_w = -\sqrt{\frac{\nu U_w}{x}} f(0) \quad (10)$$

represents the mass transfer at the surface with $V_w > 0$ for injection and $V_w < 0$ for suction. We further assume the stretching velocity $U_w(x,t)$, surface temperature $T_w(x,t)$, and concentration at the surface $C_w(x,t)$ in the following forms:

$$U_w(x,t) = \frac{ax}{1-ct}, \quad T_w(x,t) = T_\infty + \frac{bx}{1-ct}, \quad C_w(x,t) = C_\infty + \frac{ex}{1-ct}, \quad (11)$$

in which a, b, e, and c are constants with $a > 0$, $b \geq 0$, $e \geq 0$, and $c \geq 0$ with $ct < 1$. We choose a time dependent magnetic field [32–36] $B(t) = B_0(1-ct)^{-1}$ and a time dependent reaction rate $R(t) = R_0(1-ct)^{-1}$ with B_0 and R_0 as the uniform magnetic field and reaction rate, respectively.

We introduce

$$\eta = \sqrt{\frac{U_w}{\nu x}}y, \quad \psi = \sqrt{\nu x U_w} f(\eta), \quad \theta(\eta) = \frac{T - T_\infty}{T_w - T_\infty}, \quad \phi(\eta) = \frac{C - C_\infty}{C_w - C_\infty}, \quad (12)$$

and the velocity components

$$u = \frac{\partial \psi}{\partial y} \quad v = -\frac{\partial \psi}{\partial x}, \quad (13)$$

where ψ is a stream function. The continuity equation is identically satisfied and the resulting problems for f, θ, and ϕ become

$$f''' + ff'' - f'^2 - A\left(f' + \frac{1}{2}\eta f''\right) - M^2 f' = 0, \quad (14)$$

$$\frac{1}{Pr}\left(1 + \frac{4}{3}R_d\right)\theta'' + f\theta' - \theta f' - A\left(\theta + \frac{1}{2}\eta\theta'\right) = 0, \quad (15)$$

$$\frac{1}{Sc}\phi'' + f\phi' - \phi f' - \gamma\phi - A\left(\phi + \frac{1}{2}\eta\phi'\right) = 0, \quad (16)$$

$$f(0) = S, \quad f'(0) = 1, \quad \theta(0) = 1,$$
$$\phi(0) = 1, \quad f'(\eta) \to 0, \quad \theta(\eta) \to 0, \quad (17)$$
$$\phi(\eta) \to 0, \quad \eta \to \infty,$$

with $f(0) = S$ which for $S < 0$ corresponds to suction case and $S > 0$ implies injection. Here $A = c/a$ is an unsteadiness parameter and for $A = 0$ the problem reduce to the steady state situation. The Hartman number M, the Prandtl number Pr, the radiation parameter R_d, the Schmidt number Sc and the chemical reaction parameter γ are, respectively, given by

$$M^2 = \frac{\sigma B_0^2}{\rho a}, \quad Pr = \frac{\mu c_p}{k}, \quad R_d = \frac{4\sigma^* T_\infty^3}{k^* k}, \quad Sc = \frac{\nu}{D}, \quad \gamma = \frac{R_0}{a}, \quad (18)$$

and the prime denotes the derivative with respect to η.

Expressions of the skin friction coefficient C_f, local Nusselt number Nu_x, and the surface mass transfer ϕ' at the wall are defined as

$$C_f = \frac{\tau_w}{\rho U_w^2/2}, \quad Nu_x = \frac{xq_w}{k(T_w - T_\infty)}, \quad \phi'(0) = \left(\frac{\partial \phi}{\partial y}\right)_{y=0} \leq 0, \quad (19)$$

where the skin friction τ_w and the heat transfer q_w from the plate are

$$\tau_w = \mu\left(\frac{\partial u}{\partial y}\right)_{y=0}, \quad q_w = -\left[\left(k + \frac{16\sigma^* T_\infty^3}{3k^*}\right)\frac{\partial T}{\partial y}\right]_{y=0}. \quad (20)$$

In terms of dimensionless variables we have

$$\frac{1}{2}C_\mathrm{f}\mathrm{Re}_x^{1/2} = f''(0),\quad Nu_x\mathrm{Re}_x^{-1/2}\left(\frac{4}{4+3R_\mathrm{d}}\right) = -\theta'(0). \tag{21}$$

3. Homotopy Analysis Solutions

The velocity $f(\eta)$, the temperature $\theta(\eta)$, and the concentration fields $\phi(\eta)$ can be expressed by the set of base functions

$$\left\{\eta^k \exp(-n\eta)|k \geq 0,\ n \geq 0\right\} \tag{22}$$

in the form

$$f(\eta) = a_{0,0}^0 + \sum_{n=0}^{\infty}\sum_{k=0}^{\infty} a_{m,n}^k \eta^k \exp(-n\eta), \tag{23}$$

$$\theta(\eta) = \sum_{n=0}^{\infty}\sum_{k=0}^{\infty} b_{m,n}^k \eta^k \exp(-n\eta), \tag{24}$$

$$\phi(\eta) = \sum_{n=0}^{\infty}\sum_{k=0}^{\infty} c_{m,n}^k \eta^k \exp(-n\eta), \tag{25}$$

where $a_{m,n}^k$, $b_{m,n}^k$, and $c_{m,n}^k$ are the coefficients. Based on the rule of solution expressions and the boundary conditions (17), one can choose the initial guesses f_0, θ_0, and ϕ_0 of $f(\eta)$, $\theta(\eta)$, and $\phi(\eta)$ as

$$f_0(\eta) = 1 + S - \exp(-\eta), \tag{26}$$

$$\theta_0(\eta) = \exp(-\eta), \tag{27}$$

$$\phi_0(\eta) = \exp(-\eta), \tag{28}$$

and the auxiliary linear operators are expressed by the following equations:

$$\mathcal{L}_f = \frac{\mathrm{d}^3 f}{\mathrm{d}\eta^3} - \frac{\mathrm{d}f}{\mathrm{d}\eta}, \tag{29}$$

$$\mathcal{L}_\theta = \frac{\mathrm{d}^2\theta}{\mathrm{d}\eta^2} - \theta, \tag{30}$$

$$\mathcal{L}_\phi = \frac{\mathrm{d}^2\phi}{\mathrm{d}\eta^2} - \phi. \tag{31}$$

Note that the above operators possess the following properties:

$$\mathcal{L}_f\left[C_1 + C_2\exp(\eta) + C_3\exp(-\eta)\right] = 0, \tag{32}$$

$$\mathcal{L}_\theta\left[C_4\exp(\eta) + C_5\exp(-\eta)\right] = 0, \tag{33}$$

$$\mathcal{L}_\phi\left[C_6\exp(\eta) + C_7\exp(-\eta)\right] = 0, \tag{34}$$

where C_i $(i = 1-7)$ are arbitrary constants.

If $p \in [0,1]$ is the embedding parameter and $\hbar_f$, $\hbar_\theta$, and $\hbar_\phi$ indicate the non-zero auxiliary parameters, respectively, then the zeroth-order deformation problems are

$$(1-p)\mathcal{L}_f[\hat{f}(\eta,p) - f_0(\eta)] = p\hbar_f\mathcal{N}_f[\hat{f}(\eta,p)], \tag{35}$$

$$(1-p)\mathcal{L}_\theta[\hat{\theta}(\eta,p) - \theta_0(\eta)] = p\hbar_\theta\mathcal{N}_\theta[\hat{f}(\eta,p),\hat{\theta}(\eta,p)], \tag{36}$$

$$(1-p)\mathcal{L}_\phi[\hat{\phi}(\eta,p) - \phi_0(\eta)] = p\hbar_\phi\mathcal{N}_\phi[\hat{f}(\eta,p),\hat{\phi}(\eta,p)] \tag{37}$$

with the boundary conditions

$$\hat{f}(\eta;p)\big|_{\eta=0} = S,\quad \left.\frac{\partial\hat{f}(\eta;p)}{\partial\eta}\right|_{\eta=0} = 1,\quad \left.\frac{\partial\hat{f}(\eta;p)}{\partial\eta}\right|_{\eta=\infty} = 0, \tag{38}$$

$$\hat{\theta}(\eta;p)\big|_{\eta=0} = 1,\quad \hat{\theta}(\eta;p)\big|_{\eta=\infty} = 0, \tag{39}$$

$$\hat{\phi}(\eta;p)\big|_{\eta=0} = 1,\quad \hat{\phi}(\eta;p)\big|_{\eta=\infty} = 0, \tag{40}$$

and the nonlinear operators $\mathcal{N}_f$, $\mathcal{N}_\theta$, and $\mathcal{N}_\phi$ are

$$\begin{aligned}\mathcal{N}_f\left[\hat{f}(\eta;p)\right] &= \frac{\partial^3\hat{f}(\eta,p)}{\partial\eta^3} + \hat{f}(\eta,p)\frac{\partial^2\hat{f}(\eta,p)}{\partial\eta^2} - \left(\frac{\partial\hat{f}(\eta,p)}{\partial\eta}\right)^2 - M^2\frac{\partial\hat{f}(\eta,p)}{\partial\eta}\\ &\quad - A\left(\frac{\partial\hat{f}(\eta,p)}{\partial\eta} + \frac{1}{2}\eta\frac{\partial^2\hat{f}(\eta,p)}{\partial\eta^2}\right),\end{aligned} \tag{41}$$

$$\begin{aligned}\mathcal{N}_\theta\left[\hat{\theta}(\eta;p),\hat{f}(\eta;p)\right] &= \left(1 + \frac{4}{3}R_\mathrm{d}\right)\frac{\partial^2\hat{\theta}(\eta,p)}{\partial\eta^2} + Pr\left(\hat{f}(\eta,p)\frac{\partial\hat{\theta}(\eta,p)}{\partial\eta} - \frac{\partial\hat{f}(\eta;p)}{\partial\eta}\hat{\theta}(\eta;p)\right)\\ &\quad - APr\left(\hat{\theta}(\eta;p) + \frac{1}{2}\eta\frac{\partial\hat{\theta}(\eta,p)}{\partial\eta}\right),\end{aligned} \tag{42}$$

$$\begin{aligned}\mathcal{N}_\phi\left[\hat{\phi}(\eta;p),\hat{f}(\eta;p)\right] &= \frac{\partial^2\hat{\phi}(\eta;p)}{\partial\eta^2} + Sc\left(\hat{f}(\eta,p)\frac{\partial\hat{\phi}(\eta;p)}{\partial\eta} - \frac{\partial\hat{f}(\eta;p)}{\partial\eta}\hat{\phi}(\eta;p) - \gamma\hat{\phi}(\eta;p)\right)\\ &\quad - ASc\left(\hat{\phi}(\eta;p) + \frac{1}{2}\eta\frac{\partial\hat{\phi}(\eta;p)}{\partial\eta}\right).\end{aligned} \tag{43}$$

For $p=0$ and $p=1$, we have

$$\hat{f}(\eta;0)=f_0(\eta), \quad \hat{f}(\eta;1)=f(\eta), \tag{44}$$

$$\hat{\theta}(\eta;0)=\theta_0(\eta), \quad \hat{\theta}(\eta;1)=\theta(\eta), \tag{45}$$

$$\hat{\phi}(\eta;0)=\phi_0(\eta), \quad \hat{\phi}(\eta;1)=\phi(\eta). \tag{46}$$

Expanding $\hat{f}(\eta;p)$, $\hat{\theta}(\eta;p)$, and $\hat{\phi}(\eta;p)$ in Taylor's theorem with respect to an embedding parameter p, one has

$$\hat{f}(\eta;p)=f_0(\eta)+\sum_{m=1}^{\infty} f_m(\eta)p^m, \tag{47}$$

$$\hat{\theta}(\eta;p)=\theta_0(\eta)+\sum_{m=1}^{\infty} \theta_m(\eta)p^m, \tag{48}$$

$$\hat{\phi}(\eta;p)=\phi_0(\eta)+\sum_{m=1}^{\infty} \phi_m(\eta)p^m, \tag{49}$$

$$\begin{aligned} f_m(\eta) &= \frac{1}{m!}\frac{\partial^m f(\eta;p)}{\partial\eta^m}\bigg|_{p=0}, \\ \theta_m(\eta) &= \frac{1}{m!}\frac{\partial^m \theta(\eta;p)}{\partial\eta^m}\bigg|_{p=0}, \\ \phi_m(\eta) &= \frac{1}{m!}\frac{\partial^m \phi(\eta;p)}{\partial\eta^m}\bigg|_{p=0}. \end{aligned} \tag{50}$$

The auxiliary parameters are so properly chosen that the series (47) – (49) converge at $p=1$, then we have

$$f(\eta)=f_0(\eta)+\sum_{m=1}^{\infty} f_m(\eta), \tag{51}$$

$$\theta(\eta)=\theta_0(\eta)+\sum_{m=1}^{\infty} \theta_m(\eta), \tag{52}$$

$$\phi(\eta)=\phi_0(\eta)+\sum_{m=1}^{\infty} \phi_m(\eta). \tag{53}$$

The mth-order deformation problems are

$$\mathcal{L}_f\left[f_m(\eta)-\chi_m f_{m-1}(\eta)\right]=\hbar_f\mathcal{R}_m^f(\eta), \tag{54}$$

$$\mathcal{L}_\theta\left[\theta_m(\eta)-\chi_m \theta_{m-1}(\eta)\right]=\hbar_\theta\mathcal{R}_m^\theta(\eta), \tag{55}$$

$$\mathcal{L}_\phi\left[\phi_m(\eta)-\chi_m \phi_{m-1}(\eta)\right]=\hbar_\phi\mathcal{R}_m^\phi(\eta), \tag{56}$$

$$\begin{aligned} &f_m(0)=0,\ f'_m(0)=0,\ f'_m(\infty)=0, \\ &\theta_m(0)=0,\ \theta_m(\infty)=0,\ \phi_m(0)=0,\ \phi_m(\infty)=0, \end{aligned} \tag{57}$$

$$\begin{aligned} &\mathcal{R}_m^f(\eta)= \\ &f'''_{m-1}-M^2 f'_{m-1}-A\left[f'_{m-1}+\frac{1}{2}\eta f''_{m-1}\right] \\ &+\sum_{k=0}^{m-1}\left[f_{m-1-k}f''_k-f'_{m-1-k}f'_k\right], \end{aligned} \tag{58}$$

$$\begin{aligned} &\mathcal{R}_m^\theta(\eta)= \\ &\left(1+\frac{4}{3}R_\mathrm{d}\right)\theta''_{m-1}-APr\left[\theta_{m-1}+\frac{1}{2}\eta\theta'_{m-1}\right] \\ &+Pr\sum_{k=0}^{m-1}\left[f_{m-1-k}\theta'_k-\theta_{m-1-k}f'_k\right], \end{aligned} \tag{59}$$

$$\begin{aligned} &\mathcal{R}_m^\phi(\eta)= \\ &\phi''_{m-1}-Sc\gamma\phi_{m-1}-ASc\left[\phi_{m-1}+\frac{1}{2}\eta\phi'_{m-1}\right] \\ &+Sc\sum_{k=0}^{m-1}\left[f_{m-1-k}\phi'_k-\phi_{m-1-k}f'_k\right], \end{aligned} \tag{60}$$

$$\chi_m=\begin{cases}0, & m\le 1,\\ 1, & m>1.\end{cases} \tag{61}$$

The general solutions of (54) – (57) are

$$f_m(\eta)=f_m^*(\eta)+C_1+C_2\exp(\eta)+C_3\exp(-\eta), \tag{62}$$

$$\theta_m(\eta)=\theta_m^*(\eta)+C_4\exp(\eta)+C_5\exp(-\eta), \tag{63}$$

where $f_m^*(\eta)$, $\theta_m^*(\eta)$, and $\phi_m^*(\eta)$ denote the special solutions and

$$\begin{aligned} &C_2=C_4=C_6=0, \quad C_1=-C_3-f_m^*(0), \\ &C_3=\frac{\partial f^*(\eta)}{\partial\eta}\bigg|_{\eta=0}, \\ &C_5=-\theta_m^*(0), \quad C_7=-\phi_m^*(0). \end{aligned} \tag{64}$$

Note that (54) – (56) can be solved by Mathematica one after the other in the order $m=1,2,3,\ldots$

4. Convergence of the Homotopy Solutions

The analytical series solutions (51) – (53) contain the non-zero auxiliary parameters $\hbar_f$, $\hbar_\theta$, and $\hbar_\phi$ which can adjust and control the convergence of the series solutions. In order to see the range of admissible values of $\hbar_f$, $\hbar_\theta$, and $\hbar_\phi$ of the functions $f''(0)$, $\theta'(0)$, and $\phi'(0)$ the $\hbar_f$, $\hbar_\theta$, and $\hbar_\phi$-curves are displayed for 25th-order of approximations. It is obvious from Figure 1 that the range for the admissible values of $\hbar_f$, $\hbar_\theta$, and $\hbar_\phi$ are $-0.8\le\hbar_f\le-0.3$, $-1.5\le\hbar_\theta\le-0.3$,

Table 1. Convergence of HAM solution for different order of approximations.

Order of approximation	$-f''(0)$	$-\theta'(0)$	$-\phi'(0)$
1	1.46875	0.83542	1.93750
5	1.78492	0.73571	1.80378
10	1.80191	0.72477	1.80242
15	1.80242	0.72338	1.80242
20	1.80242	0.72314	1.80242
25	1.80242	0.72310	1.80242
27	1.80242	0.72309	1.80242
30	1.80242	0.72309	1.80242

(a)

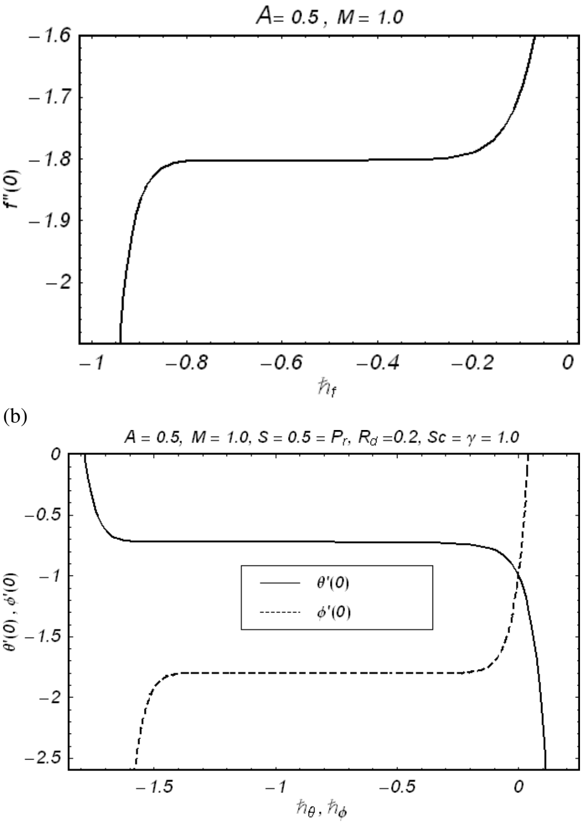

Fig. 1. $\hbar$-curves for 25th-order of approximations.

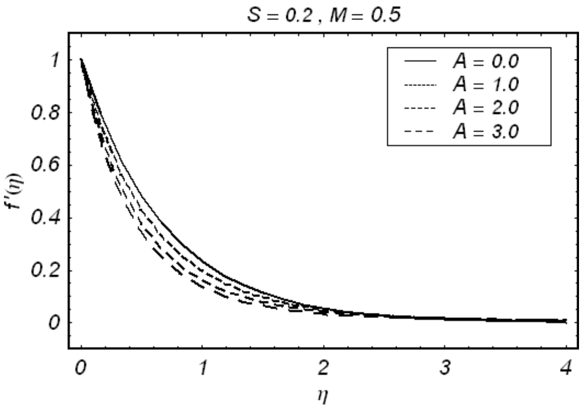

Fig. 2. Influence of A on the velocity f'.

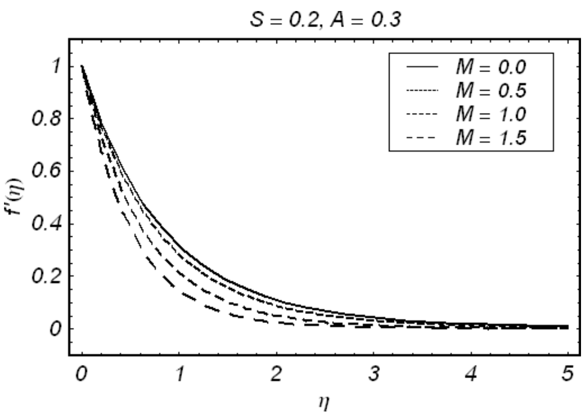

Fig. 3. Influence of M on the velocity f'.

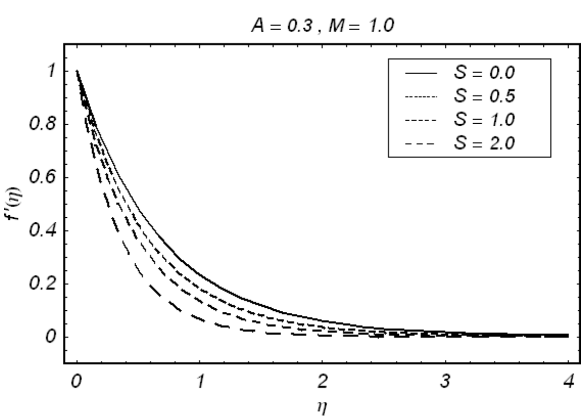

Fig. 4. Influence of S on the velocity f'.

and $-1.4 \leq \hbar_\phi \leq -0.1$. It is found from our computations that the series given by (51)–(53) converge in the whole region of η when $\hbar_f = -0.6$ and $\hbar_\theta = -1 = \hbar_\phi$. Table 1 shows the convergence of the homotopy solutions for different order of approximations as $A = 0.5$, $M = 1.0$, $S = 0.5 = Pr$, $R_\mathrm{d} = 0.2$, $Sc = \gamma = 1.0$.

5. Discussion of the Results

This section deals with the variations of Hartman number M, unsteadiness parameter A, the suction parameter S, the Prandtl number Pr, radiation parameter R_d, the Schmidt number Sc, and the chemical reaction parameter γ on the velocity f', the concentration ϕ, and the temperature fields θ. Figures 2–4 represent the variations of A, M, and S on f'. Figure 2 describes the

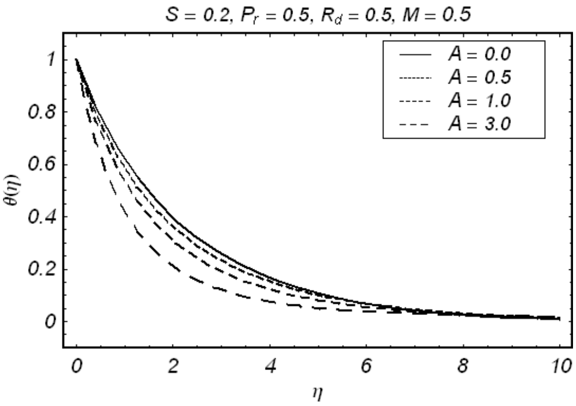

Fig. 5. Influence of A on the temperature θ.

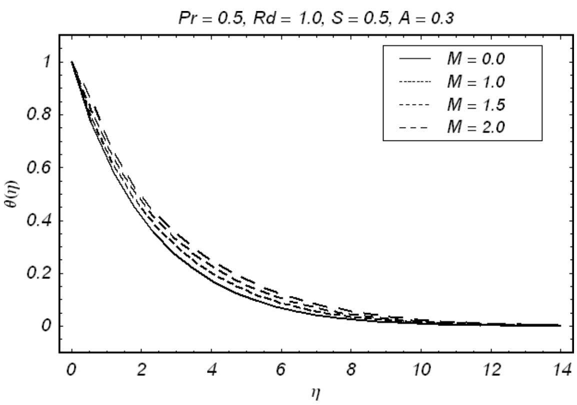

Fig. 6. Influence of M on the temperature θ.

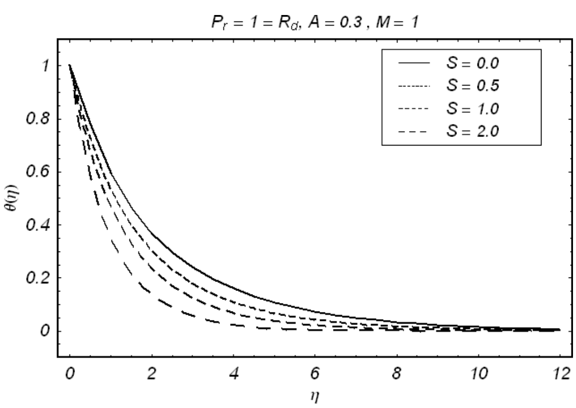

Fig. 7. Influence of S on the temperature θ.

effect of A on f'. It is noticed that f' decreases when A increases. Figures 3 and 4 show the effects of M and S on f', respectively. Obviously f' is a decreasing function of M and S.

Figures 5 – 9 depict the influences of A, M, S, Pr, and R_d on θ. Figure 5 indicates that θ decreases as

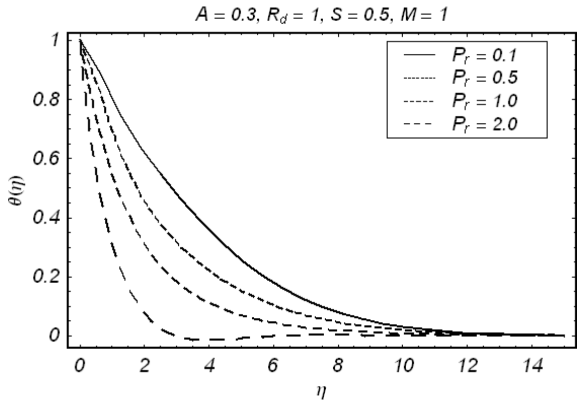

Fig. 8. Influence of Pr on the temperature θ.

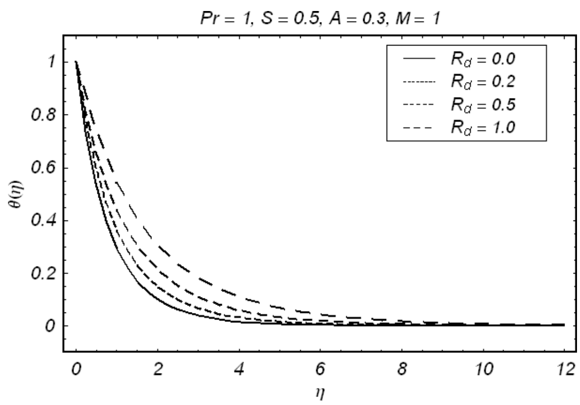

Fig. 9. Influence of R_d on the temperature θ.

A increases. Figure 6 gives the behaviour of M on θ. The temperature profile increases as M increases. Figure 7 elucidates the influence of S on θ. The temperature field θ decreases when S increases. It is observed that θ decreases when Pr increases (Fig. 8). Figure 9 describes the effects of R_d on θ. Here θ increases as R_d increases.

Figures 10 – 15 are plotted for the effects of A, M, S, Sc, and γ on the concentration field ϕ. It is seen from Figure 10 that ϕ decreases as the unsteadiness parameter increases. Figure 11 depicts the concentration field ϕ for various values of M. Here ϕ increases for large M. Figure 12 shows the variation of S on the concentration field ϕ. Clearly, ϕ is a decreasing function of S and the concentration boundary layer thickness also decreases when S increases. The variation of Schmidt number Sc on ϕ is shown in Figure 13. The concentration field ϕ decreases by increasing Sc. The concentration boundary layer thickness also decreases for large values of Sc. Figure 14 displays the

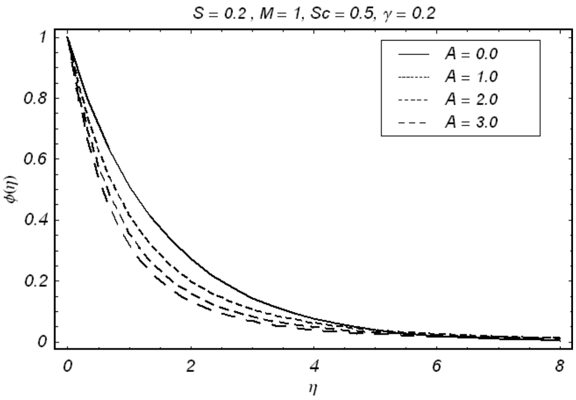

Fig. 10. Influence of *A* on the concentration ϕ.

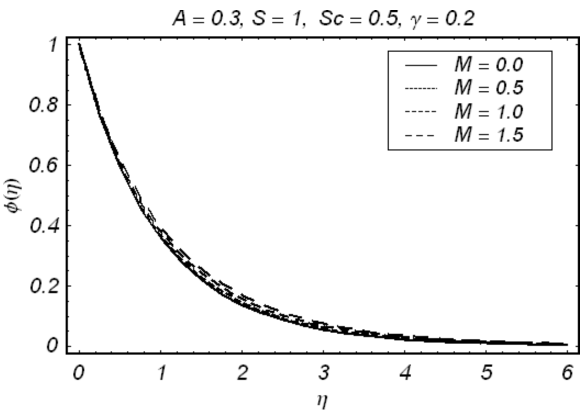

Fig. 11. Influence of *M* on the concentration ϕ.

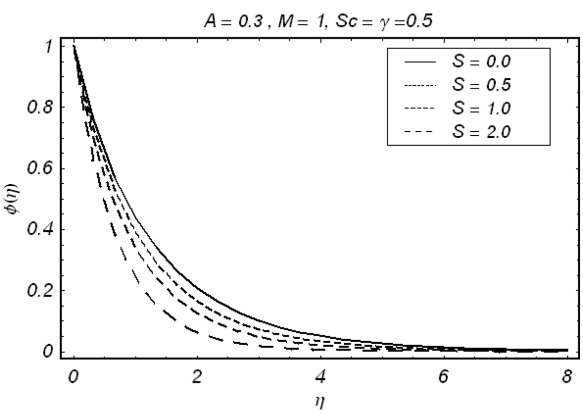

Fig. 12. Influence of *S* on the concentration ϕ.

influence of the destructive chemical reaction parameter $(\gamma > 0)$ on the concentration profile ϕ. It is obvious that the fluid concentration decreases with an increase in the destructive chemical reaction parameter. Figure 15 illustrates the effect of the generative chemical reaction parameter $(\gamma < 0)$ on the concentration profile ϕ. This figure illustrates that the concentration field ϕ has a opposite behaviour for $\gamma < 0$ when compared with the case of the destructive chemical reaction parameter $(\gamma > 0)$.

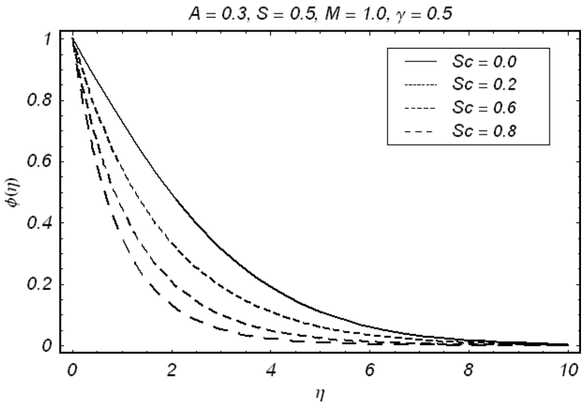

Fig. 13. Influence of *Sc* on the concentration ϕ.

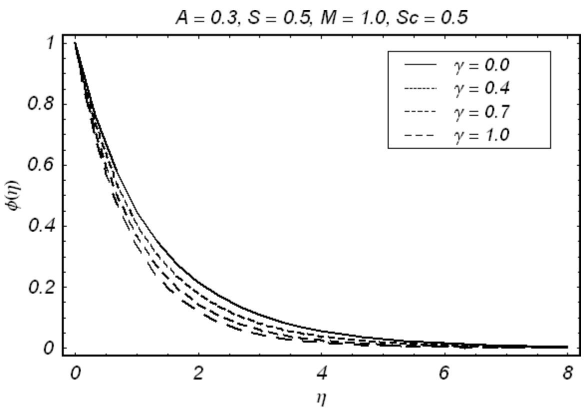

Fig. 14. Influence of $\gamma\ (> 0)$ on the concentration ϕ.

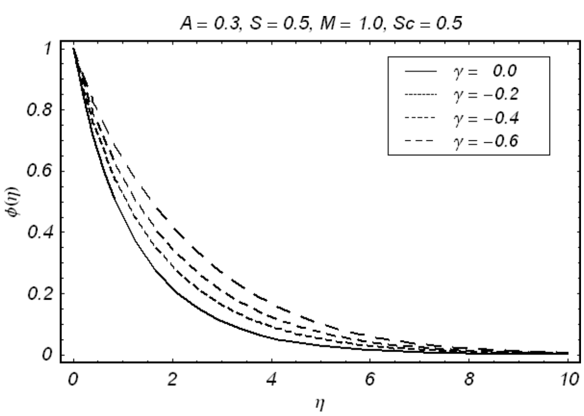

Fig. 15. Influence of $\gamma\ (< 0)$ on the concentration ϕ.

Table 2. Values of skin friction coefficient $\frac{1}{2}C_f\mathrm{Re}_x^{1/2}$ for the parameters A, M, and S.

A	M	S	$-\frac{1}{2}C_f\mathrm{Re}_x^{1/2}$
0	1.2	0.5	1.831929
0.3			1.896669
0.7			1.980895
1.5			2.042426
0.3	0		1.372527
	0.5		1.479822
	1.0		1.756433
	1.5		2.127268
	2		2.547232
	1.2	0	1.631209
		0.2	1.732803
		0.7	2.013439
		1.0	2.199467

Table 3. Values of $-\theta'(0)$ for some values of A, S, and Pr when $M = R_\mathrm{d} = 0$.

A	S	Pr	[15]	[15]	HAM
0	−1.5	0.72	0.4570268328	0.4570	0.4570269
		1	0.5000000000	0.5000	0.5000000
		10	0.654161289	0.6542	0.6451651
	0	0.72	0.8086313498	0.8086	0.8086313
		1	1.0000000000	1.0000	1.0000000
		3	1.923682594	1.9237	1.9235912
		10	3.720673901	3.7207	3.7215965
	1.5	0.72	1.494368413	1.4944	1.4943687
		1	2.000000000	2.0000	2.0000731
1	−1.5	1		0.8095	0.8095322
	0			1.3205	1.3205523
	2			2.2224	2.2223645

Table 1 is prepared for the convergence of the series solutions. It is found that in $\phi'(0)$ the convergence is achieved at 10th-order of approximations, for $f''(0)$ it is at 15th-order of approximations, and at 27th-order approximation in $\theta'(0)$. Table 2 includes the values of the skin friction coefficient $\frac{1}{2}C_f\mathrm{Re}_x^{1/2}$. It is noticed that the magnitude of the skin friction coefficient increases for large values of A, M, and S. Table 3 depicts the variation of the heat transfer characteristic at the wall $-\theta'(0)$ when $M = 0 = R_\mathrm{d}$, and for different values of A, S, and Pr. From this table one can see that the HAM solution is in good agreement with an exact solution [15]. Table 4 presents the values of $-\theta'(0)$ for some values of A, M, R_d when $Pr = 0.5 = S$. The magnitude of $-\theta'(0)$ increases for large M and R_d. However, it it increases for larger values of A. Table 5 consists of the surface mass transfer $-\phi'(0)$ for different values of A, M, S, Sc, and γ. It is apparent from this table that the magnitude of $-\phi'(0)$ increases for large values of A and S, and decreases for large values of M. The magnitude of $-\phi'(0)$ increases when Sc and γ increases.

Table 4. Values of $-\theta'(0)$ for some values of A, M, and R_d when $Pr = 0.5 = S$.

A	M	R_d	$-\theta'(0)$
0.4	1	0.2	0.69411
0.5			0.72338
0.8			0.80061
1.1			0.86834
1.5			0.94861
0.3	1.2		0.64979
	1.4		0.63665
	2		0.60151
	2.5		0.57780
	1	0.1	0.71902
		0.3	0.61683
		0.5	0.54402
		0.7	0.48901

Table 5. Values of mass transfer $-\phi'(0)$ for some values of A, M, S, Sc, and γ.

A	M	S	Sc	γ	$-\phi'(0)$
0	1.2	0.5	1	1	1.67337
0.3					1.74525
0.7					1.83828
1.5					2.01409
0.3	0				1.79047
	0.5				1.78036
	1				1.75643
	2				1.70025
	1.2	0			1.47762
		0.2			1.57953
		0.5			1.74524
		1			2.05246
		0.5	0.2		0.65248
			0.7		1.39621
			1.2		1.95861
			2		2.72023
			1	0.3	1.45282
				0.6	1.58870
				1.3	1.91605
				2	2.06823
				5	2.57039

6. Conclusions

This article presents the series solution for the unsteady two dimensional flow bounded by a stretching surface. Emphasis in this study is given to the unsteadiness, radiation, MHD, and mass transfer effects. The salient features of present analysis are reproduced below.

- The variations of M, A, and S on f' are qualitatively similar.
- Effects of A, Pr, and S on θ are similar.
- The behaviours of M and R_d on θ are opposite to that of A, Pr, and S.

• Variation of M on θ and ϕ is similar whereas reverse trend is noted for f'.

• Effects of S and A on f', θ, and ϕ are similar in the qualitative sense.

• The variation of Sc on ϕ is similar to that of $\gamma > 0$ and is opposite to $\gamma < 0$.

• Variations of A on the magnitudes of skin friction coefficients and local Nusselt number and mass transfer are similar.

• Effects of M on the magnitudes of mass transfer and local Nusselt number is same but is different for the skin friction coefficient.

• Variations of M and R_{d} on the magnitude of the local Nusselt number are the same. However, such variations of M and R_{d} on the local Nusselt number are quite different than that of A.

• Effect of S on the magnitudes of skin friction coefficient and the mass transfer is same.

Acknowledgements

We are grateful to the referees for their fruitful comments and suggestions.

[1] S. J. Liao, Fluid Mech. **488**, 189 (2003).
[2] Z. Abbas and T. Hayat, Int. J. Heat Mass Transfer **51**, 1024 (2008).
[3] R. Cortell, Int. J. Nonlinear Mech. **41**, 78 (2006).
[4] M. Sajid and T. Hayat, Int. Commun. Heat Mass Transfer **35**, 347 (2008).
[5] P. D. Ariel, T. Hayat, and S. Ashgar, Acta Mech. **187**, 29 (2006).
[6] A. Ishak, R. Nazar, and I. Pop, Heat Mass Transfer **44**, 921 (2008).
[7] T. Hayat, Z. Abbas, and M. Sajid, Theor. Comput. Fluid Dyn. **20**, 229 (2006).
[8] R. Cortell, Phys. Lett. A **372**, 631 (2008).
[9] S. J. Liao, Int. J. Heat Mass Transfer **48**, 2529 (2005).
[10] A. Ishak, R. Nazar, and I. Pop, J. Eng. Math. **62**, 23 (2008).
[11] C. D. S. Devi, H. S. Takhar, and G. Nath, Heat Mass Transfer **26**, 71 (1991).
[12] H. I. Andersson, J. B. Aarseth, and B. S. Dandapat, Int. J. Heat Mass Transfer **43**, 69 (2003).
[13] R. Nazar, N. Amin, and I. Pop, Mech. Res. Commun. **31**, 121 (2004).
[14] S. J. Liao, Commun. Nonlinear Sci. Numer. Simul. **11**, 326 (2006).
[15] A. Ishak, R. Nazar, and I. Pop, Nonlinear Analysis: Real World Appl. **10**, 2909 (2009).
[16] S. J. Liao, Beyond perturbation: Introduction to homotopy analysis method, Chapman and Hall, CRC Press, Boca Raton 2003.
[17] S. J. Liao, Appl. Math. Comput. **147**, 499 (2004).
[18] T. Hayat and Z. Abbas, ZAMP **59**, 124 (2008).
[19] S. Abbasbandy, Phys. Lett. A **360**, 109 (2006).
[20] A. S. Bataineh, M. S. M. Noorani, and I. Hashim, Phys. Lett. A **372**, 613 (2008).
[21] W. Wu and S. J. Liao, Chaos, Solitons and Fractals **26**, 117 (2005).
[22] T. Hayat, Z. Abbas, and T. Javed, Phys. Lett. A **372**, 637 (2008).
[23] T. Hayat and Z. Abbas, Chaos, Solitons and Fractals **38**, 556 (2008).
[24] A. S. Bataineh, M. S. M. Noorani, and I. Hashim, Commun. Nonlinear Sci. Numer. Simul. **14**, 409 (2009).
[25] S. J. Liao, Commun. Nonlinear Sci. Numer. Simulat. **14**, 2144 (2009).
[26] T. Hayat, T. Javed, and Z. Abbas, Nonlinear Analysis: Real World Appl. **10**, 1514 (2009).
[27] T. Hayat, Z. Abbas, and N. Ali, Phys. Lett. A **372**, 4698 (2008).
[28] S. Abbasbandy, Chem. Eng. J. **136**, 114 (2008).
[29] T. Hayat and Z. Abbas, Chaos Soliton and Fractals **38**, 556 (2008).
[30] M. Sajid, T. Javed, and T. Hayat, Nonlinear Dyn. **51**, 259 (2008).
[31] M. M. Ali, T. S. Chen, and B. F. Armaly, AIAA J. **22**, 1797 (1984).
[32] T. Hayat, H. Mambili-Mamboundou, E. Momoniat, and F. M. Mahomed, J. Nonlinear Math. Phys. **15**, 77 (2008).
[33] T. Hayat, E. Momaniat, and F. M. Mahomed, Int. J. Modern Phys. B **22**, 2489 (2008).
[34] M. B. Abd-el-Malek, N. A. Bardan, and H. S. Hassan, Int. J. Eng. Sci. **40**, 1599 (2002).
[35] M. Subhas Abel, N. Mahesha, and J. Tawade, Appl. Math. Model. **33**, 3430 (2009).
[36] C. W. Soh, Commun. Nonlinear Sci. Numer. Simul. **10**, 537 (2005).